

# Dynamics of Stable-Unstable Switching of a Laser Diode Subject to Feedback

Jia-Xin Dong<sup>1</sup>, Song-Sui Li<sup>2</sup>, and Sze-Chun Chan<sup>1,2,\*</sup>

<sup>1</sup>Department of Electronic Engineering, City University of Hong Kong, Hong Kong, China

<sup>2</sup>State Key Laboratory of Millimeter Waves, City University of Hong Kong, Hong Kong, China

\*Email: scchan@cityu.edu.hk

**Abstract**—A laser diode subject to optical feedback in the long-cavity regime is experimentally investigated for its intrinsic switching dynamics. The intensity time series of the single-mode distributed-feedback laser is monitored as the feedback strength is adjusted. The laser is observed to dynamically switch between a stable state and an unstable state, which is oscillatory around the relaxation resonance frequency of the laser. The stable-unstable switching repeats in every feedback delay time with a tunable duty cycle for a clear burst of microwave oscillation on the laser emission intensity. According to the optical spectra, the switching dynamics is a result of gain competition between stable and unstable states at different optical frequencies. According to the power spectra, a clear envelope of the microwave frequency components is observed in correspondence to the duty cycle. The stable-unstable switching is amongst the other well-studied dynamics such as regular pulsing, quasi-periodicity, and chaos in lasers with feedback.

## 1. Introduction

Semiconductor lasers subject to perturbations are well-known for exhibiting various nonlinear dynamics [1-3]. The perturbations can be implemented by optical injection from another laser, delayed optical feedback from the laser itself, or electrical feedback after photodetection. Among these schemes, optical feedback has been appealing to many studies because of its simplicity as well as the diversity of the triggered nonlinear dynamics [4-10]. In a semiconductor laser with delayed optical feedback, it has been established that nonlinear dynamics such as stable emission, period-one oscillation, regular pulse packages, and chaos can be observed [4-10]. These dynamics allow applications including microwave generation, random bit generation, and secure communication [2, 3]. Some special dynamics were reported as consisting of more than one state under the same operating condition. For example, bistability has been observed between regular pulse packages and other states [11], polarization modes in edge-emitting lasers [12], as well as polarization modes in vertical-cavity surface-emitting lasers [13].

In this work, we experimentally investigate an intrinsic dynamics switching between a stable state and an unstable state for a single-mode laser diode subject to optical feedback in the long-cavity regime. A clear burst of microwave

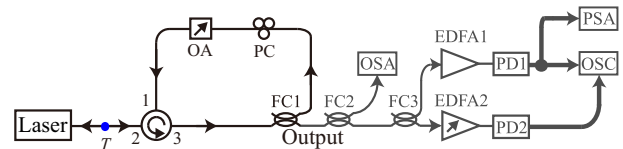


Figure 1: Schematic of a laser diode subject to feedback in the long-cavity regime. FC, fiber coupler; OA, variable optical attenuator; PC, polarization controller; EDFA, erbium-doped fiber amplifier; PD, photodetector; OSC, oscilloscope; PSA, power spectrum analyzer; OSA, optical spectrum analyzer.

oscillation on the laser emission intensity is obtained by the stable-unstable switching in every feedback delay time. The switching is related to gain competition between stable and unstable states at different optical frequencies. A clear envelope of the microwave frequency components in the power spectra is also observed as dependent on the tunable duty cycle of the switching. The stable-unstable switching is potentially applicable in photonic microwave generation [14]. It resembles the chimera states in optoelectronic oscillators with electronic feedback [15, 16]. This switching dynamics adds to the other well-studied dynamics such as regular pulsing, quasi-periodicity, and chaos in lasers with feedback.

## 2. Experiment

Figure 1 schematically shows the experimental setup of a semiconductor laser subject to optical feedback. The laser is a 1.55- $\mu\text{m}$  single-mode distributed-feedback laser (FITEL FRL15DCW5-A81-19327). It has a threshold of about 10 mA when temperature-stabilized at 21 °C. The laser is biased at 50 mA to result in an output power of 9 mW as measured at position  $T$  in Fig. 1. Its free-running optical frequency is  $\nu_0 = 193.47$  THz before the feedback is applied. Light emitted from the laser passes through a packaged fiber pigtail with a nominal coupling efficiency of 0.5. It is then coupled into a circulator via port 2. After the circulator, a fiber coupler FC1 splits 30% of the power for monitoring and detection. The remaining 70% of the power passes through a polarization controller and a variable optical attenuator. Then, the light returns into the laser cavity through the circulator via port 1 and 2. As a result, a

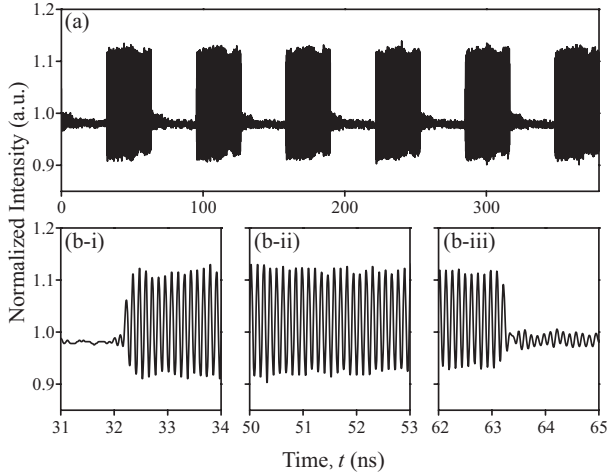


Figure 2: Normalized intensity time series for the output of the laser shown in time windows of (a)  $6\tau$  and (b) 3 ns, where details are presented for the (i) beginning, (ii) middle, and (iii) end of the occurrence of the unstable oscillatory state. The feedback power  $P$  is  $88 \mu\text{W}$ .

feedback loop is formed with a delay time of  $\tau = 63$  ns. The feedback is regarded as in the long-cavity regime as the delay time is much longer than the reciprocal of the relaxation resonance frequency of the laser. The polarization controller matches the polarizations of the feedback light and the laser cavity. The attenuator enables the tuning of the feedback power  $P$  as measured at position  $T$ . Two 50:50 fiber couplers FC2 and FC3 are used for the subsequent monitoring and detection of the output from the laser. One arm of FC2 is monitored by an optical spectrum analyzer (YOKOGAWA AQ6370), while the other arm is connect to FC3 for detection by an ac-coupled 50-GHz photodetector PD1 (u2t XPDV2120RA) and a dc-coupled 1.2-GHz photodetector PD2 (Thorlabs DET01CFC). The detectors are used with preamplification by an erbium-doped fiber amplifier EDFA1 with a fixed output power of 20 mW and a variable erbium-doped fiber amplifier EDFA2. Practically, PD2 is used for calibrating the output of PD1 for its intensity offset and responsivity. The two time series from the photodetectors are recorded by a 12-GHz real-time oscilloscope (Agilent DSO90254A). The signal from PD1 is also split for monitoring by a power spectrum analyzer (Agilent N9010A) incorporating a microwave amplifier (Agilent 83006A).

### 3. Results and Discussion

To begin with, the feedback power  $P$  is kept below 0.1 nW, so that the laser is essentially in the free-running state. Then, by reducing the attenuation of the attenuator in Fig. 1,  $P$  is gradually increased to  $88 \mu\text{W}$ , where bursts of oscillation at a microwave frequency occurs repeatedly in the emission intensity time series in Fig. 2(a). The time

intensity series in Fig. 2 is normalized to the free-running intensity. The laser switches between a stable state and an unstable state with the oscillatory intensity at a microwave frequency of about 8.35 GHz. The microwave oscillation is modulated by a temporal envelope with the form of a rectangular function with a duty cycle  $\eta$  of about 0.5. The repetition period of the switching is 63 ns corresponding to the feedback delay time  $\tau$ . Figure 2(b) gives zoomed views of the first oscillation burst in Fig. 2(a) for its (i) beginning, (ii) middle, and (iii) end. The laser quickly enters the oscillation state from the stable state with the transition completed within a few oscillations in Fig. 2(b-i). The laser maintains in oscillation with the intensity varying from 0.91 to 1.11 in Fig. 2(b-ii), though slight fluctuations due to noise is also observed. The laser then ends the oscillation at time near 63 ns in Fig. 2(b-iii), where the oscillation amplitude quickly reduces. Although residual oscillation is observed in Fig. 2(b-iii) immediately after 63 ns, its amplitude soon reduces to zero as the laser returns to the stable state according to Fig. 2(a). To help understand the mechanism behind this switching dynamics, the optical frequency components that contribute to the stable and the unstable states should be elucidated as follows.

In the frequency domain, the optical spectra and the corresponding electrical power spectra are shown in Fig. 3, where the feedback power  $P$  is set at (a)  $106 \mu\text{W}$ , (b)  $97 \mu\text{W}$ , (c)  $94 \mu\text{W}$ , and (d)  $88 \mu\text{W}$ . The optical spectra in Fig. 3(i) with a limited resolution bandwidth of 2.5 GHz are offset to the free-running frequency  $\nu_0$ . In Fig. 3(a-i), the duty cycle  $\eta$  of the unstable state is only 0.05, so the stable state dominates the spectrum with a component at  $\nu_s$  being much stronger than the other components. In fact,  $\nu_s$  is slightly below  $\nu_0$  and thus receives much gain of the laser. For every cycle of  $\tau$ ,  $\nu_s$  only switches off momentarily for  $0.05\tau$  with the rise of a set of frequency components including  $\nu_p$ ,  $\nu_+$ , and  $\nu_-$  as marked by the gray lines, which are equally separated by  $f_0$ . The stable and unstable oscillatory states do not coexist simultaneously [14]. Nonetheless, compared to the switching time on the order of nanoseconds, the sweep time of the optical spectrum analyzer is too slow for temporally resolving the optical frequency components of the stable and unstable states. The beat signal of the optical frequency components in Fig. 3(a-i) is presented by the power spectrum in Fig. 3(a-ii). Strong components arise in low-frequency region due to the switching at  $\tau$ . Strong components are also observed  $f_0 = 8.12$  GHz due to the beating of  $\nu_p$ ,  $\nu_+$ , and  $\nu_-$ , while the second harmonic at  $2f_0$  is observable as well. The power spectrum offset to  $f_0$  is shown in Fig. 3(a-iii). The frequency components are densely packed with a separation of  $1/\tau = 15.8$  MHz. Interestingly, a clear spectral envelope is observed on these frequency components. The envelope resembles a sinc-function that diminishes to zero at  $(0.05\tau)^{-1}$ , which is consistent with the Fourier transform of the square-wave envelope in the intensity time series.

As the feedback power  $P$  gradually reduces in Fig. 3(a-i)

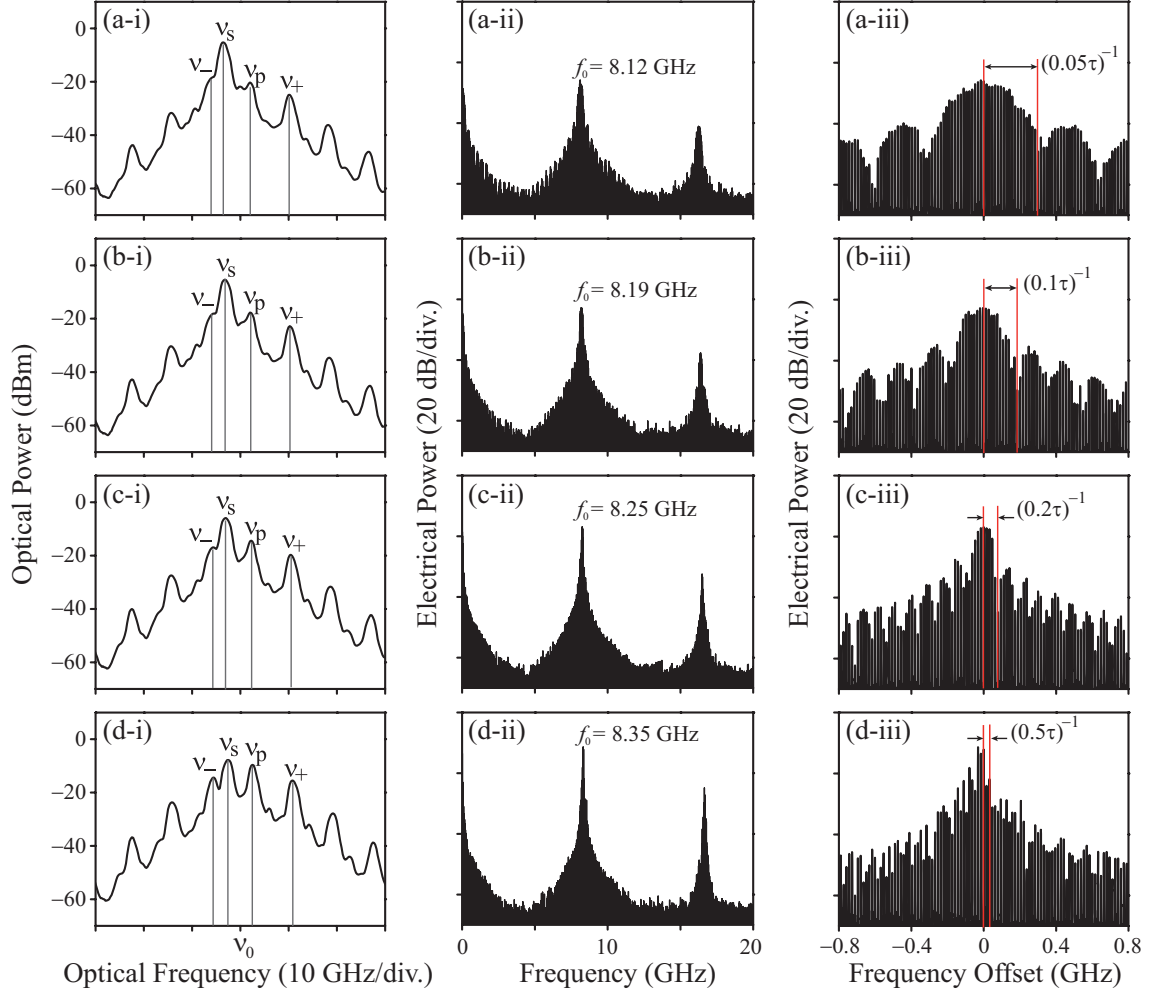


Figure 3: (i) Optical spectra centered at the free-running frequency  $\nu_0$ , (ii) power spectra in the full span, and (iii) power spectra in a reduced span with frequency offset to  $f_0$  for the output of the laser. The feedback power  $P$  is set at (a)  $106 \mu\text{W}$ , (b)  $97 \mu\text{W}$ , (c)  $94 \mu\text{W}$ , and (d)  $88 \mu\text{W}$ , which correspond to a switching duty cycle of  $\eta$  of 0.05, 0.1, 0.2, and 0.5, respectively.

to Fig. 3(d-i), the power of  $\nu_s$  continually weakens while  $\nu_p$  strengthens. This is a result of the gain competition in the laser, which corresponds to the increment of  $\eta$  from 0.05 to 0.5. Specifically, with the strengthening of  $\nu_p$  in Fig. 3(d-i), the associated sidebands at  $\nu_-$  and  $\nu_+$  are strengthened. All of the three components  $\nu_p$ ,  $\nu_+$ , and  $\nu_-$  can be clearly identified. It should be noted that Fig. 3(d) corresponds to the time series shown in Fig. 2 with  $\eta = 0.5$ . Besides, although the feedback power  $P$  affects the power of the optical frequency components, it does not strongly influence the beat frequency  $f_0$  of the unstable state, according to Figs. 3(a-ii) to Fig. 3(d-ii). It is observed that  $f_0$  only increases slightly from 8.12 GHz to 8.35 GHz, while the microwave power at  $f_0$  increases as  $\eta$  increases. In addition, according to Figs. 3(a-iii) to Fig. 3(d-iii), the central lobe of the spectral envelope reduces in width as  $\eta$  increases.

#### 4. Conclusion

In conclusion, we have demonstrated the switching between a stable state and an unstable oscillatory state in a semiconductor laser subject to feedback in the long-cavity regime. When the feedback strength is properly adjusted, the laser enters the stable-unstable switching. The stable-unstable switching corresponds to repeated bursts of microwave oscillation of the emission intensity in every feedback delay time. Competition for gain between the two states corresponds to the variation of optical power for the optical frequency components of the stable and unstable states. The resultant tunability of the duty cycle is also observable in the spectral envelope of the power spectrum. This switching dynamics is of potential in photonic microwave generation.

## Acknowledgments

The work described in this work was fully supported by the Research Grants Council of Hong Kong, China (CityU 11201014, 11260916, and T42-103/16-N).

## References

- [1] M. Sciamanna and K. A. Shore, “Physics and applications of laser diode chaos,” *Nat. Photon.*, vol. 9, pp. 151–162, 2015.
- [2] M. C. Soriano, J. Garcia-Ojalvo, C. R. Mirasso, and I. Fischer, “Complex photonics: Dynamics and applications of delay-coupled semiconductor lasers,” *Rev. Mod. Phys.*, vol. 85, p. 421, 2013.
- [3] A. Uchida, K. Amano, M. Inoue, K. Hirano, S. Naito, H. Someya, I. Oowada, T. Kurashige, M. Shiki, S. Yoshimori, K. Yoshimura, and P. Davis, “Fast physical random bit generation with chaotic semiconductor lasers,” *Nat. Photon.*, vol. 2, pp. 728–732, 2008.
- [4] R. Lang and K. Kobayashi, “External optical feedback effects on semiconductor injection laser properties,” *IEEE J. Quantum Electron.*, vol. 16, pp. 347–355, 1980.
- [5] M. Yousefi, D. Lenstra, and G. Vemuri, “Nonlinear dynamics of a semiconductor laser with filtered optical feedback and the influence of noise,” *Phys. Rev. E*, vol. 67, p. 046213, 2003.
- [6] S. G. Abdulrhmann, M. Ahmed, T. Okamoto, W. Ishimori, and M. Yamada, “An improved analysis of semiconductor laser dynamics under strong optical feedback,” *IEEE J. Sel. Top. Quantum Electron.*, vol. 9, pp. 1265–1274, 2003.
- [7] A. K. Dal Bosco, Y. Akizawa, K. Kanno, A. Uchida, T. Harayama, and K. Yoshimura, “Photonic integrated circuits unveil crisis-induced intermittency,” *Opt. Express*, vol. 24, pp. 22198–22209, 2016.
- [8] S. Donati and R. H. Horng, “The diagram of feedback regimes revisited,” *IEEE J. Sel. Top. Quantum Electron.*, vol. 19, pp. 1500309–1500309, 2013.
- [9] S. S. Li and S. C. Chan, “Chaotic time-delay signature suppression in a semiconductor laser with frequency-detuned grating feedback,” *IEEE J. Sel. Top. Quantum Electron.*, vol. 21, pp. 541–552, 2015.
- [10] D. Brunner, R. Luna, A. D. i Latorre, X. Porte, and I. Fischer, “Semiconductor laser linewidth reduction by six orders of magnitude via delayed optical feedback,” *Opt. Lett.*, vol. 42, pp. 163–166, 2017.
- [11] A. Tabaka, K. Panajotov, I. Veretennicoff, and M. Sciamanna, “Bifurcation study of regular pulse packages in laser diodes subject to optical feedback,” *Phys. Rev. E*, vol. 70, p. 036211, 2004.
- [12] T. Heil, I. Fischer, W. Elsäßer, and A. Gavrielides, “Dynamics of semiconductor lasers subject to delayed optical feedback: The short cavity regime,” *Phys. Rev. Lett.*, vol. 87, p. 243901, 2001.
- [13] D. W. Sukow, T. Gilfillan, B. Pope, M. S. Torre, A. Gavrielides, and C. Masoller, “Square-wave switching in vertical-cavity surface-emitting lasers with polarization-rotated optical feedback: Experiments and simulations,” *Phys. Rev. A*, vol. 86, p. 033818, 2012.
- [14] J. X. Dong, J. P. Zhuang, S. C. Chan, “Tunable switching between stable and periodic states in a semiconductor laser with feedback,” manuscript submitted for publication.
- [15] A. F. Talla, R. Martinenghi, P. Wofo, and Y. K. Chembo, “Breather and Pulse-Package Dynamics in Multinonlinear Electrooptical Systems With Delayed Feedback,” *IEEE Photon. J.*, vol. 8, pp. 1–8, 2016.
- [16] L. Larger, B. Penkovsky, and Y. Maistrenko, “Laser chimeras as a paradigm for multistable patterns in complex systems,” *Nat. Commun.*, vol. 6, p. 7752, 2015.